UNIVERSITA' DEGLI STUDI DI
MILANO-BICOCCA

Scuola di Scienze Matematiche Fisiche e Naturali
Corso di laurea Triennale in Fisica

PROBING OPTICAL AND RADIO-LOUD AGN FRACTIONS : A COMPARATIVE ANALYSIS BETWEEN BCGs AND NON-BCGs SAMPLES at z < 0.1

Candidate:
Andrea Maccarinelli

Supervisor:
Prof. Sebastiano Cantalupo

Co-supervisors:
Dott. Andrea Travascio

anno accademico 2022/2023

Abstract

Brightest cluster galaxies (BCGs) are the most massive and luminous galaxies located near the center of relaxed, virialized, and undisturbed galaxy clusters in the local Universe ([1, 2]). According to several observational studies ([3, 4]), these objects experience a special formation process differing from general galaxy evolution.

Current theoretical models (e.g., [5, 6]) predict that dry mergers are the dominant mechanisms responsible for their mass assembly at $z < 1$. These objects are often observed to host a supermassive black hole (SMBH) in their center ([7]). The process of matter accretion into these SMBHs may release a large amount of energy, resulting in Active Galactic Nuclei (AGN). There are two primary modes in which SMBH accretion can occur: the so-called 'quasar mode' and the 'radio mode'. The quasar mode involves a high accretion rate of the SMBH via an optically- thick and geometrically-thin disk, with most of the energy being released in the form of radiation. In a radio mode scenario, the SMBH accretion of gas occurs at a low rate in an optically-thin and geometrically-thick disk configuration, releasing energy in the form of relativistic particles, i.e. radio jets. The latter is typically observed in BCGs.

The evolutionary processes of BCGs are still not fully understood, and there are no specific studies comparing the frequency of different types of AGN in BCGs with respect to other types of galaxies (e.g., [8]). The main scientific question guiding my thesis project is to investigate whether the different evolution of BCGs, coupled with their "special" environment, promotes the accretion of SMBHs in their centers compared to other types of galaxies in the local universe, at $z < 0.1$. To address this question, I analyzed a sample of BCGs within the redshift range of z = 0.02-0.1. This sample was derived from the combination of the Sloan Digital Sky Survey Data Release 7 (SDSS DR7 [9]) and the C4 BCGs catalogue produced by [10, 11]. I utilized

the flux measurements of optical emission lines i.e. $H\alpha$, [OIII], $H\beta$, [NII], and [SII] doublets by the MPA-JHU team. These fluxes were estimated using methods outlined in [12]. This allowed me to conduct a selection of optical AGN through the [NII]- and [SII]- BPT diagnostic diagrams [13]. Additionally, I conducted a cross-matching of the aforementioned catalogs with a dataset obtained from [14], where the spectroscopic sample of the SDSS DR2 was cross- correlated with catalogs of galaxies observed from the National Radio Astronomy Observatory (NRAO) Very Large Array (VLA) Sky Survey (NVSS; [15]) and the Faint Images of the Radio Sky at Twenty centimeters (FIRST) survey [16]. Using this new catalog of BCGs probed with these radio surveys, I was able to select the BCGs that exhibit radio loudness. Following this classification, I finally estimated the fraction of BCGs classified as Optical and Radio Loud AGN. Subsequently, I derived these fractions for a sample of non-BCG selected galaxies using the same procedure employed to obtain the BCG catalog.

These analyses reveal that BCGs exhibit a higher fraction of Optical AGN $\sim 50\%$ compared to the non-BCG sample, which shows a percentage of $\sim 21\%$, consistent with the results found by [17]. Simultaneously, the analysis of Radio Loud emissions indicates that BCGs are more inclined to host Radio Loud Activity, with a fraction of $\sim 12\%$. This fraction is found to be 20 times higher than the fraction observed in the non-BCG sample of selected galaxies, which is $\sim 0.6\%$.

In conclusion, these results demonstrate that BCGs are more likely to host optical AGN activity and radio-loud emission compared to other types of galaxies. This suggests that their privileged position facilitates frequent accretion of SMBHs in both accretion modes. Previous studies, such as [10, 18, 19] have already shown a prevalence of radio AGN among the BCG population in the local Universe. However, few studies (e.g., [8]) have attempted to compare the distribution of BCGs in BPT diagrams to that of normal galaxies. The fact that the fraction of AGN is greater for special galaxies is both expected and interesting to understand the nature of these objects. Future studies will aim to test the results obtained with this sample and to understand if this higher fraction is specifically driven by differences in properties between BCGs and non-BCGs, such as mass, star formation rate, metallicity, and kinematics.

Contents

Chapter 1

Introduction

1.1 The Active Galactic Nuclei

Active galaxies constitute a distinctive class characterized by an intensely energetic source at their center, known as an Active Galactic Nucleus (AGN). Since the first observation of an active galaxy in the early 1900s, numerous studies have been conducted on this intriguing category of galaxies. To this day, efforts persist in unraveling the nature and role of active galaxies within the broader context of galactic formation and evolution.

Research in this field has demonstrated that the intense radiation must emanate from a compact region, with a spatial dimension not exceeding 100 parsecs. This estimation was derived from the temporal variability observed in some of these sources [20]. Additionally, it has been noted that AGNs exhibit luminosity variations of over 50% within timescales ranging from days to years. Such fluctuations can only be explained if a substantial portion of the emission region is randomly connected. These observations strongly imply that the central component of AGNs is likely a Supermassive Black Hole (SMBH), namely a rapidly accreting black hole.

AGN emissions span the entire electromagnetic spectrum, with variations in the different components depending on the classification of the observed nuclei. Despite these differences in emissions, a General Model known as the "Unified model" can still be defined, which applies to each classification of AGNs. [21]

In addition to the previously mentioned supermassive black hole (SMBH) at the center, there is an accreting disk located in close proximity, serving as a primary source of UV radiation. The central region, excluding the

disk, is the main contributor to X-rays, while gas clouds orbiting near the BH give rise to Broad Emission Lines, forming what is known as the Broad Line Region (BLR). In the outer regions, situated both above and below the accreting disk, the primary contributor to Narrow Emission Lines, thus defining the Narrow Line Region (NLR), is the presence of diffuse gas. Additionally, surrounding the disk, there's a toroidal-shaped volume composed of a mixture of gas and dust, leading to the partial absorption of central radiation.

The final torus-shaped volume is indeed one of the main reasons for explaining the extreme variety observed in active galaxies and the different modes in which SMBH growth occurs. From a historical perspective, AGNs are divided into two main categories: Type 1 and Type 2, with the addition of Blazars. According to the 'Unified Model,' the main difference between these categories is merely apparent, arising from nothing more than variations in the observer's line of sight and the presence of the obscuring torus.

- **Type I:** The emission lines exhibit a broad component, typically in the range of $\sim 10^3$-$10^4, \mathrm{km\ s^{-1}}$, along with a narrow component. In this configuration, the observer is situated at a small angle relative to the torus axis, allowing the radiation from circumnuclear regions to remain unobscured along the line of sight
- **Type II:** Emission lines exhibit only a narrow component, typically not exceeding $1200, \mathrm{km\ s^{-1}}$. In this scenario, the line of sight intersects the obscuring matter of the torus.
- **Blazars:** In this scenario, the observer's line of sight is closely aligned with the axis of the radio jets emanating from the source.

The substantial energy released during the accretion process of a SMBH by an AGN plays a significant role in shaping the evolution of the host galaxy. In this context, the literature often discusses positive and negative feedback mechanisms, which correspond to different physical phenomena such as radiation pressure, jet generation, and winds. Positive feedback occurs when active nuclei promote stellar formation, while negative feedback involves the suppression of star formation.

In the literature, various theoretical models of galactic evolution can be found, referring to physical mechanisms capable of heating gas on immense

scales ($>> 1kpc$), as proposed by Di Matteo et al. (2005). These models are also capable of halting star formation and consequently depositing metals into the surrounding environment, as suggested by Gebhardt et al. (2000).

The most accepted theory predicts that winds generated by accretion onto the SMBH can be responsible for both mechanisms of quenching or enhancing star formation.

Two distinct AGN feedback mechanisms have been proposed, each associated with different rates of mass accretion onto the SMBH (Fabian, 2012; Harrison, 2017).

- **QSO's Radiative Feedback :** This feedback mode, often referred as quasar mode consists in a high accretion rate of the SMBH via an optically-thick and geometrically-thin disk, and most of the energy is released in form of radiation.
- **QSO's Radio Feedback :** In this scenario, the SMBH accretion of hotter gas happens with a low rate in a optically-thin and geometrically-thick disk configuration, releasing energy in form of relativistic particles. such as Radio Jets.

1.2 The Brightest Cluster Galaxies

The Hierarchical model stands as a cornerstone in our understanding of cosmic structure formation, delineating the principal pathways through which galaxies burgeon in both stellar luminosity and mass. At its core, this model elucidates how galaxies amass their content by drawing in and assimilating matter from their surroundings.

One of the most extreme examples in this context involves the study of Brightest Cluster Galaxies (BCGs), a unique class of galaxies, often situated at the center and typically standing out as the most luminous and massive objects within the entire cluster.(e.g. [22]).

Considering their environment, observational studies, such as [4], have indicated that the evolution of Brightest Cluster Galaxies (BCGs) differs from the normal galactic path. The prevailing model for cosmic structure formation (i.e. the Cold Dark Matter Model) suggests that the mass assembly of BCGs is primarily influenced by dry mergers [5, 6].

At low redshift, these objects exhibit a small dispersion in their aperture luminosities and, indeed, have been frequently chosen as standard candles

for cosmological tests throughout the literature, also because of the shared properties with the cluster itself.

Mainly found to be Elliptical galaxies, BCGs seems to not be drawn from the same luminosity function as normal elliptic objects outside the cluster environment, and in general has been proven to differ also from generic Bright galaxies. (i.e. [23])

Due to their distinct evolutionary histories, the primary mechanism driving the mass growth of galaxies is associated with cooling flows within lower mass halos at high redshifts. However, at low redshifts, this phenomenon diminishes, primarily due to increased Active Galactic Nuclei (AGN) activity accreting mass into their typically hosted SMBH [7].

As presented before regarding AGN feedback, also BCGs are interested by both of the Quasi Stellar Object modes, resulting in Optical AGN, and Radio Loud Emission such as Radio Jets(e.g. [10]).

These relativistic jets of radio emission are also recognized as one of the main explanation of the so called "Cooling flow problem". The unique relaxed and virialized environment defining the cluster often has cooling time-scales much shorter than Hubble time, that following to the absence of a heating source would lead to the presence of a cooling flow.

However observational studies found that temperature of cluster cores fails to fall below $\sim 30\%$ at large radii resulting in an amount of cooling gas corresponding only to the $\sim 10\%$ expected from the existent cooling flow model. [24]

1.3 The Aim of this thesis

In this context, the main scientific question driving this work is to understand **whether the different evolution of BCGs, along with their "special" environment, affects the accretion of SMBHs in their centers compared to other types of galaxies in the local universe**.

In particular, this study will present a comparative analysis between two representative samples of BCGs and Non-BCGs to highlight the substantial differences that the cluster environment induces in SMBH accretion.

To address this particular inquiry, I conducted an analysis on a BCG sample compiled from the Sloan Digital Sky Survey Data Release 7 (SDSS DR7), as outlined in [9], and the C4 BCGs catalogue created by [10]. For this specific BCG sample, I utilized the optical line fluxes ($H\alpha$, [OIII], $H\beta$, [NII], and [SII] doublets) provided by the MPA-JHU team to establish a comprehensive understanding of optical AGN presence through the [NII]- and [SII]- BPT diagnostic diagrams. Furthermore, through cross-matching these aforementioned catalogs with datasets derived from NVSS and FIRST radio surveys, as outlined in [14], I identified BCGs displaying radio loud emission, indicative of the existence of radio jets.

These analyses, including data description in subsection 2.1 "Data description" and data analysis in subsection 2.2 "Data analysis," will be comprehensively presented in the "Methods" chapter.

Following the "Methods" chapter, the subsequent section will delve into the third chapter, concentrating on the disclosure of the acquired outcomes.

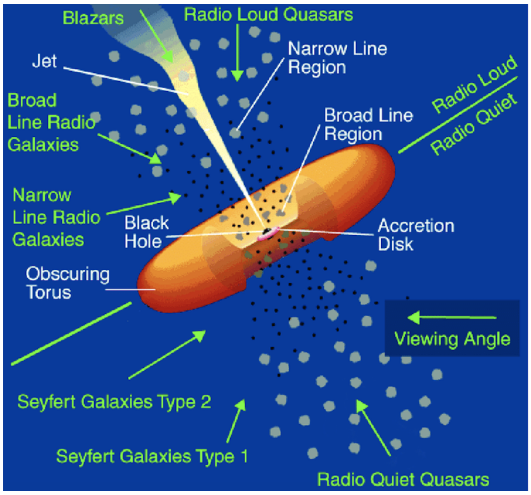

Figure 1.1: The Unified AGN model as proposed in [21]

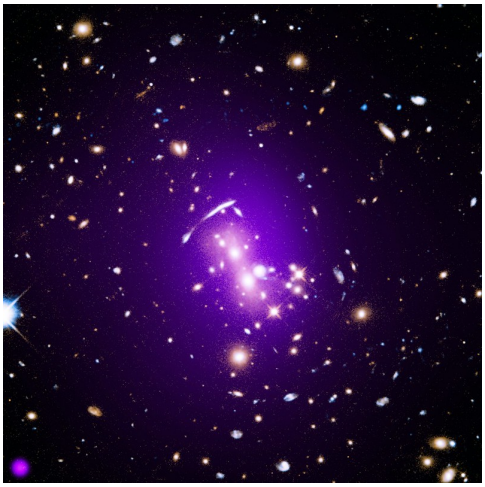

Figure 1.2: This image of galaxy cluster SPT-CLJ0310-464 X-rays from Chandra are shown along with optical data from Hubble

Chapter 2

Methods

The study of cosmic objects, such as galaxies, relies on the analysis of the electromagnetic spectrum emanating from these distant sources. Within a spectrum, various pieces of information can be extracted, with the primary focus being on the intensity of light across a range of energies or frequencies. A crucial aspect of a spectrum involves determining the intensity at specific wavelengths.

This thesis will concentrate on utilizing specific information derived from spectra (e.g., flux, flux error) associated with both permitted and forbidden emission lines. In a galactic context, particularly within a galaxy cluster, the continuum originates from the diffuse light emitted by stars. On the other hand, emission lines, which are prominently observed in such environments, are typically generated by elements like Hydrogen, Helium, Oxygen, etc.

There are various methods to investigate the electromagnetic spectrum, with the two primary branches being Spectroscopy and Photometry.

Astrophysical spectroscopy is a fundamental tool used to analyze the electromagnetic radiation emitted or absorbed by celestial objects. By examining the spectral lines and features, it is possible to mine important informations such as chemical composition, temperature, density etc.

On the other hand, photometry measures the overall brightness of celestial objects across different wavelength bands, providing information about the spectral distribution of their luminous emission.

In this Thesis Work i'll be focusing on a Spectroscopic study involving the fluxes of the Forbidden Emission lines of the spectrum.

2.1 Data Description

This thesis presents results obtained through the cross-matching of three distinct celestial catalogues:

- **SDSS DR7 :** Our Main Catalogue of galaxies
- **C4-BCG :** The BCG Catalog
- **Radio Emitters :** The survey chosen for RadioLoud identification

2.1.1 SDSS DR7

The SDSS project, or Sloan Digital Sky Survey, is a comprehensive astronomical survey that maps the universe by capturing images, spectra, and photometric data of celestial objects over a large area of the sky. [9]

Funding for the project has been provided by the Alfred P. Sloan Foundation, the Participating Institutions, the National Aeronautics and Space Administration, the National Science Foundation, the U.S. Department of Energy, the Japanese Monbukagakusho, and the Max Planck Society.

This ambitious project marked its beginnings in 2000 with the goals of obtaining CCD imaging in five broad bands, covering an area of $10,000\,\mathrm{deg}^2$ of high latitude sky and spectroscopy data of a million galaxies and over 100'000 quasars over the same area.

Observations have been conducted using a a dedicated wide-field 2.5 m telescope (Gunn et al. 2006) located at Apache Point Observatory (APO) near Sacramento Peak in Southern New Mexico.

The telescope employs two distinct instruments. The first is a wide-field imager equipped with 24 tiles, each containing a 2048x2048 CCD. Imaging is performed along great circles at the sidereal rate, leading to exposure times of 54.1 seconds.

The astrometry is good to 45 milliarcseconds (mas) rms per coordinate at the bright end, while the photometric calibration is made in two modalities, respectively by tying to standard reference stars and by using the overlap between adjacent imaging runs in a process called ubercalibration.

Spectra are extracted and calibrated in terms of wavelength and flux. For galaxies near the main sample flux limit, the typical signal-to-noise ratio (S/N) is 10 per pixel. The broadband spectrophotometric calibration exhibits an accuracy of 4% root mean square (rms) for point sources

(Adelman-McCarthy et al. 2008), and the wavelength calibration is precise to 2 km s^{-1}.

The SDSS data have been made public in a series of yearly data releases, This thesis works based its results from a galactic sample derived from "Data Release 7" by the Max Planck Institute for Astrophysics and Johns Hopkins University (MPA-JHU) teams, containing the derived properties of a total of 927'552 galaxy spectra.

Physical Properties of interest :

- **Line Flux :**Flux from Gaussian fit to continuum subtracted data, corrected for foreground (galactic) reddening using techniques developed by O'Donnell [12]

- **Error Line Flux :** Developed by analyzing the duplicate observations of galaxies, to compare the empirical spread in value determinations with the random errors.

NOTA : Aggiungo un plot scat delle zone coperte da SDSS ?

2.1.2 C4 BCG Catalogue

The identification of BCGs within our primary galaxy sample, previously described, relies on the findings of A. Von der Linden et al. [10, 11]. These findings were derived from a subsequent analysis of the C4 Galaxy Cluster Catalog, initially developed by Miller et al. in 2005 [25].

The C4 catalog comprises 748 galaxy clusters identified in the Second Data Release (DR2) of the Sloan Digital Sky Survey (SDSS). Utilizing a seven-dimensional position and color space, the C4 cluster-finding algorithm identifies overdensities.

Covering approximately 2600 square degrees of the sky, the catalog spans redshifts from about 0.02 to 0.17. It includes various properties like sky location, mean redshift, galaxy membership, optical luminosity (Lr), velocity dispersion, and measures of substructure and large-scale environment.

This catalog represents one of the initial cluster catalogs constructed directly from SDSS spectroscopic data, addressing issues related to projection effects and employing mock galaxy catalogs derived from realistic N-body simulations to analyze the clustering algorithm's parameters and improve its completeness.

In this context, the work by Von Der Linden et al. [10] is noteworthy, as it builds upon the C4 catalog but introduces improved algorithms for BCG identification and measuring cluster velocity dispersion, ultimately yielding a sample of 625 BCGs.

Correcting for the SDSS photometric pipeline's tendency to underestimate luminosities in dense environments, the research refines the C4 galaxy cluster sample, addressing issues related to BCG luminosity underestimation. Given the challenges with SDSS photometry, especially for large galaxies in crowded areas, the study avoids using magnitude measurements assuming a specific profile shape.

The C4 catalog provides potential BCG candidates, but approximately 30% of clusters miss the true BCG due to fiber collisions. To address this issue, Von der Linden's team developed an algorithm to identify the BCG by estimating the virial radius, selecting the two brightest galaxies within the mean galaxy's projection, and assessing criteria such as concentration index, color compatibility, and redshift.

2.1.3 The Radio Catalogue

To investigate the radio emission characteristics of both BCGs and non-BCGs, this study conducted a crossmatch between the primary SDSS sample and a dataset comprising 2,712 radio-luminous galaxies from the work by [14]. This collection of radio-luminous objects resulted from a complex cross-matching process involving the main spectroscopic galaxy sample and two radio surveys: the National Radio Astronomy Observatories (NRAO) Very Large Array (VLA) Sky Survey (NVSS) [15] and the Faint Images of the Radio Sky at Twenty centimeters (FIRST) survey. [16]

The NVSS was the first radio survey with a sufficiently high angular resolution (45 arcsec) to allow automated cross-correlation with optical surveys. However, the FIRST catalogue offers superior angular resolution (approximately 5 arcsec), resulting in samples with much higher reliability. Nonetheless, the high angular resolution of FIRST presents its own challenges, as it is insensitive to extended radio structures and resolves out the extended emission of radio sources. Consequently, the total radio luminosity of sources larger than a few arcseconds is systematically underestimated by FIRST. To address these limitations, a hybrid approach utilizing both NVSS and FIRST surveys has been developed to identify radio sources associated with

galaxies in the SDSS spectroscopic sample. This approach capitalizes on the sensitivity of NVSS to large-scale radio structures and the high angular resolution of FIRST to reliably pinpoint the host galaxy.

The obtained radio source sample demonstrated a completeness of 95% and a reliability of 98.9%, upgrading the achievable performance of each individual survey. The sample was subsequently classified into two groups: radio-loud active galactic nuclei (AGN) and galaxies where radio emission is predominantly driven by star formation. Classification was based on a galaxy's position in the 4000-Å break strength versus radio luminosity per unit stellar mass plane, resulting in a dataset of 2,215 radio-loud AGN and 497 star-forming galaxies with radio luminosity exceeding 5 mJy at 1.4 GHz.

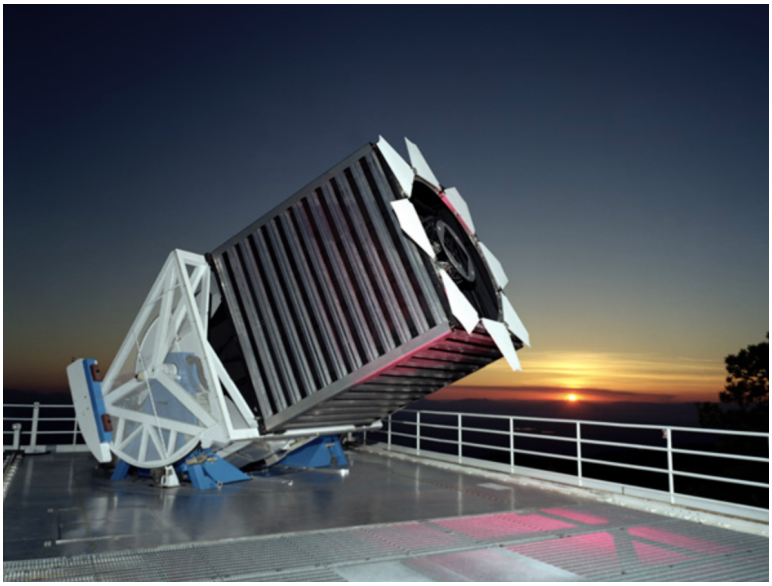

Figure 2.1: The main 2.5-meter SDSS Telescope

2.2 Data Analysis

As previously introduced, our primary galaxy sample for astrometry measurements is the MPA-JHU SDSS-derived catalogue.

The first operation required for the development of our study involved crossmatching the C4 BCG sample [11] to extract data files from the main sample, including both BCGs and non-BCGs.

This initial crossmatch was accomplished by selecting the nearest element within a radius of 2 arcsec in both RA and Dec corresponding to each of the BCGs in [11]. The result was a list of 484 corresponding selected elements.

At the end of this initial phase, the following data were collected for both samples:

- **Astrometry data:** Celestial coordinates, Redshift, Error on redshift...
- **Spectroscopy measures:** Emission lines' fluxes and their relative errors

Even though further explanation is to follow, it is preferable to introduce the second crossmatch required for this work, this time with the 2712 galaxy samples of Celestial Objects found to be active in the radio field.

In this case, the research algorithm was designed to identify the nearest correspondence within a radius of 5 arcsec. The previously created files were appropriately updated by adding a specific flag, denoted as 1, to indicate whether, when found in the Radio Sample, it implies Radio Loud Emission.

2.2.1 Optical analysis

After previously introducing the defining properties of an AGN and discussing their effects on the host galaxy, it is crucial for the subsequent optical analysis of our two samples to examine which selected objects exhibit typical properties intrinsic to the presence of an AGN. One of the primary methods employed in Astrophysics is the analysis of BPT diagnostic diagrams [13].

This type of analysis classifies different species of galaxies by scrutinizing specific ratios of emission lines produced by ionizing gas in the galaxy's Interstellar Medium (ISM), utilizing photoionization models. These specific ratios have been carefully chosen to prioritize similar wavelength fractions,

minimizing dust attenuation. Specifically, this is developed based on the following ratios:

- $\frac{[OIII]\lambda 5007}{H\beta}$
- $\frac{[SII]\lambda\lambda 6716,6731}{H\alpha}$
- $\frac{[NII]\lambda 6583}{H\alpha}$
- $\frac{[OI]\lambda 6300}{H\alpha}$

By examining these ratios, which provide evidence of different photoionization models, it is possible to draw demarcation lines and ultimately classify the final objects into different categories.

The underlying concept of this method is rooted in an intrinsic property of the ionization spectrum of massive stars near the Lyman limit of Helium, found at $\lambda = 228\mathring{A}$. Massive stars exhibit a bright cut, while the non-thermal radiation of AGNs extends to higher energies.

As a result, AGN host galaxies typically show greater ratios that surpass the demarcation lines predicted by photoionization models.

There were several photoionization models at the inception of this technique; nowadays, the preferred ones are Kauffmann et al. [26] and Kewley et al. [27].

While the ideal classification incorporates all three primary BPT diagnostics, this study relies on a classification derived solely from the BPT diagrams for [NII] and [SII].

- **BPT-[NII] Demarcation Functions:**
  - Kauffmann+03 Line:

$$\log(\frac{\text{[OIII]}}{\text{H}\beta}) = 0.61/(\log(\frac{\text{[NII]}}{\text{H}\alpha}) - 0.05) + 1.3$$

  - Kewley+01 Line:

$$\log(\frac{\text{[OIII]}}{\text{H}\beta}) = 0.61/(\log(\frac{\text{[NII]}}{\text{H}\alpha}) - 0.47) + 1.19$$

- **BPT-[SII] Demarcation Functions:**
  - Main AGN Line:

$$\log(\frac{\text{[OIII]}}{\text{H}\beta}) = 0.72/(\log(\frac{\text{[SII]}}{\text{H}\alpha}) - 0.32) + 1.30$$

– LINER/Sy2 Line:

$$\log(\frac{[\text{OIII}]}{\text{H}\beta}) = 1.89\log(\frac{[\text{SII}]}{\text{H}\alpha}) + 0.76$$

As follows it is presented a brief description of each population:

- **BPT-[NII]:**
  - **Star-forming (SF):** Below both of the demarcation lines, where the ionization is primarily from massive stars.
  - **AGN (Active Galactic Nuclei):** Above both of the demarcation lines, delineating ionization by an active nucleus.
  - **Composite:** Galaxies exhibiting a mix of both star-forming and AGN characteristics. Generally recognized to be in the area between both of the demarcation lines.
- **BPT-[SII]:**
  - **Seyferts:** Above of both of the demarcation lines, characterized by high ionization levels.
  - **LINERs (Low-Ionization Nuclear Emission Regions):** Above the Main AGN line, and below LINER/Sy2. Typically characterized by weak AGN-like ionization.
  - **Star-forming HII2:** Galaxies exhibiting ionization characteristics similar to HII regions in star-forming galaxies.

Returning to the methodology employed in this thesis, an initial screening process was conducted to exclude objects with flux values that rendered logarithmic ratios incalculable, specifically eliminating instances with numerators or denominators equal to zero. Subsequently, scatterplots were generated and demarcation lines were applied to discern distinct galaxy populations. Results images can be seen in :

Figure 2.2 Figure 2.3 Figure 2.4 Figure 2.5

Given the inclusion of error values for each flux measurement, a robust bootstrap algorithm was implemented through 5000 iterations. This algorithm introduced variations to each point on the diagnostic diagram in two

dimensions based on its probability distribution, with the mean value reflecting the error-free point and a standard deviation equivalent to the error associated with the point in both directions.

This rigorous approach facilitated an accurate determination of counts and fractions for all populations, providing a statistically refined measure of uncertainty.

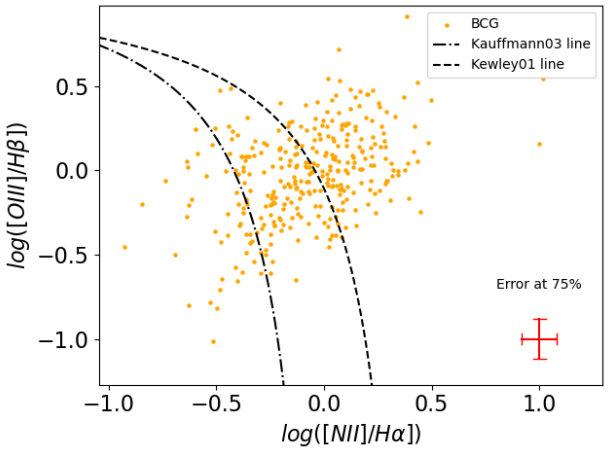

Figure 2.2: BPT NII for the BCG sample

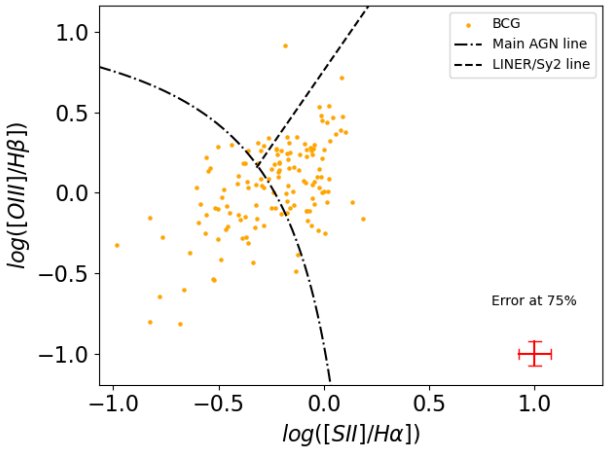

Figure 2.3: BPT SII for the BCG sample

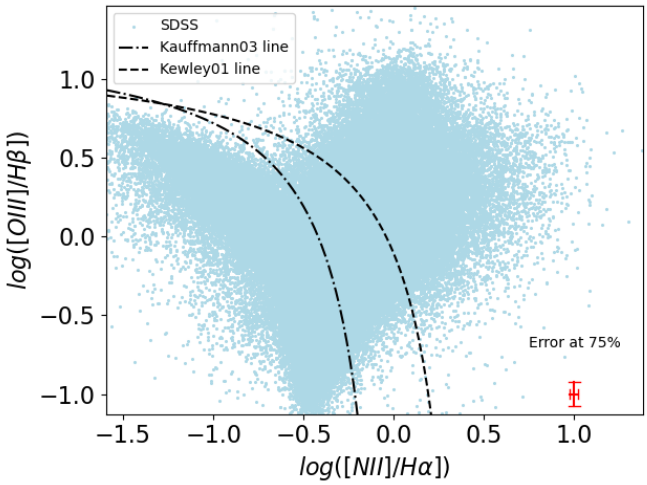

Figure 2.4: BPT NII for the SDSS noBCG sample

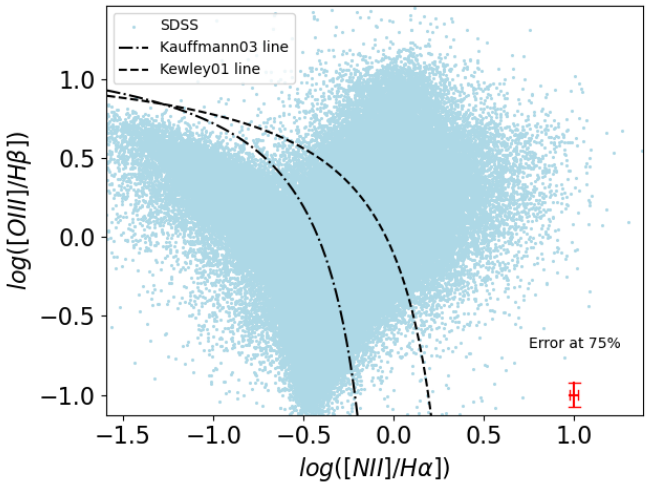

Figure 2.5: BPT SII for the SDSS noBCG sample

2.2.2 Radio Analysis

Following the preceding analyses, let's now detail how the fractions of Radio Loud AGNs were calculated for the two derived samples.

The primary goal of this analysis segment is to determine a fraction of the form :

$$\frac{N_{\text{radio}}}{N_{\text{total}}}$$

A crucial step in calculating a representative fraction of Radio Loud objects was to appropriately define the spatial regions for the fraction calculations. To accomplish this, we identified the regions mapped by the radio survey employed. Subsequently, the selection has been delineated where all three catalogs exhibited an overlap. It is essential to emphasize that the primary objective is to obtain representative fractions for both of our samples.

The selected spatial regions considered for calculating the fractions of Radio Loud objects can be found in Figure 2.6

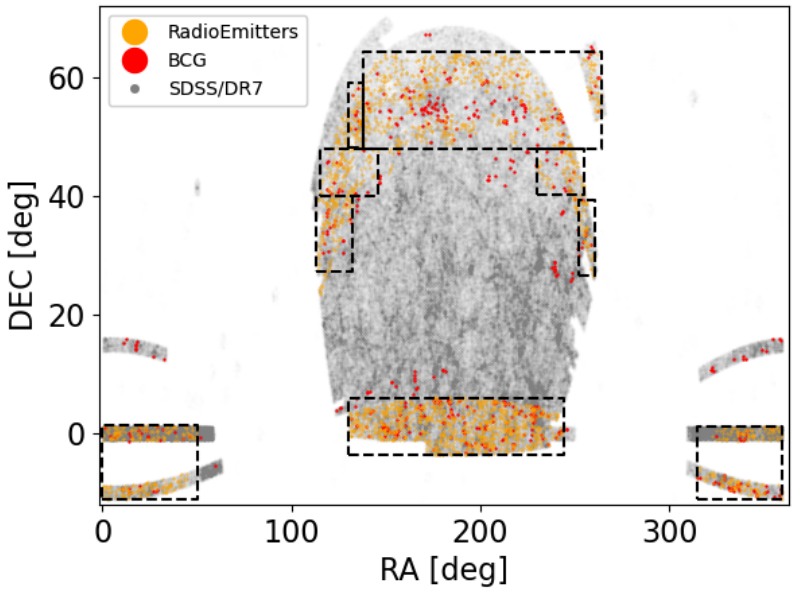

Figure 2.6: Defining Regions of Radio Loud AGN fractions

Chapter 3

Results

A complete description of the results produced !!

3.1 The Prevalence of AGN activity in BCGs

Describe how the evidence of the data analysis we conducted leads to the description of BCGs in a confrontation to non-BCGs, and in how different is still from a pure optical view the response of the AGN feedback.

Present absolutely the Table with all of the percentage (and the counting) values of the populations of both BPT NII and BPT SII diagnostics and introduce a confrontation with also the results found in Vitale et AL and others.

3.2 The Radio activity of BCGs

Explain the evidences found in the analysis and possible ways to improve results obtained.

There's certainly also the need to add a discussion on how it is possible that we ignore some of the BCGs in the counting, issue that should be resolved by choosing a more complete source of data regarding Radio Emitters galaxies.

Conclusions

The final chapter of the thesis is a summary of the work done. Therefore, in its first part it resembles much the introduction, adding to it the actual result of the work, its future evolution and prospects, in the view of the writer.

Bibliography

[1] A. Sandage and Kristian. The extension of the Hubble diagram. I. New redshifts and BVR photometry of remote cluster galaxies, and an improved richness correction. *The Astrophysical Journal*, 205:688–695, May 1976. doi: 10.1086/154324.

[2] Anja von der Linden and Wild. Star formation and AGN activity in SDSS cluster galaxies. *Monthly Notices of the Royal Astronomical Society*, 404(3):1231–1246, May 2010. doi: 10.1111/j.1365-2966.2010.16375.x.

[3] Danièl N. Groenewald and Skelton. The close pair fraction of BCGs since z = 0.5: major mergers dominate recent BCG stellar mass growth. *Monthly Notices of the Royal Astronomical Society*, 467(4):4101–4117, June 2017. doi: 10.1093/mnras/stx340.

[4] A. Travascio and Bongiorno. Multiple AGN activity during the BCG assembly of XDCPJ0044.0-2033 at z $\sim$ 1.6. *Monthly Notices of the Royal Astronomical Society*, 498(2):2719–2733, October 2020. doi: 10.1093/mnras/staa2495.

[5] Gabriella De Lucia and Jérémy Blaizot. The hierarchical formation of the brightest cluster galaxies. *Monthly Notices of the Royal Astronomical Society*, 375(1):2–14, February 2007. doi: 10.1111/j.1365-2966.2006.11287.x.

[6] Kevin C. Cooke and Kartaltepe. Stellar Mass Growth of Brightest Cluster Galaxy Progenitors in COSMOS Since z $\sim$ 3. *The Astrophysical Journal*, 881(2):150, August 2019. doi: 10.3847/1538-4357/ab30c9.

[7] D. A. Rafferty and McNamara. The Feedback-regulated Growth of Black Holes and Bulges through Gas Accretion and Starbursts in Clus-

ter Central Dominant Galaxies. *The Astrophysical Journal*, 652(1): 216–231, November 2006. doi: 10.1086/507672.

[8] S. Fisek and Alis. AGN Activity in Brigtest Cluster Galaxies (BCGs). *Communications of the Byurakan Astrophysical Observatory*, 66(2): 153–158, December 2019. doi: 10.52526/25792776-2019.66.2-153.

[9] Kevork N. Abazajian and Adelman-McCarthy. The Seventh Data Release of the Sloan Digital Sky Survey. *Astrophysical Journal Supplement Series*, 182(2):543–558, June 2009. doi: 10.1088/0067-0049/182/2/543.

[10] Anja Von Der Linden and Best. How special are brightest group and cluster galaxies? *Monthly Notices of the Royal Astronomical Society*, 379(3):867–893, August 2007. doi: 10.1111/j.1365-2966.2007.11940.x.

[11] A. von der Linden and Best. VizieR Online Data Catalog: BCG C4 cluster catalog (von der Linden+, 2007). VizieR On-line Data Catalog: J/MNRAS/379/867. Originally published in: 2007MNRAS.379..867V, July 2009.

[12] James E. O'Donnell. R v-dependent Optical and Near-Ultraviolet Extinction. *The Astrophysical Journal*, 422:158, February 1994. doi: 10.1086/173713.

[13] J. A. Baldwin, M. M. Phillips, and R. Terlevich. Classification parameters for the emission-line spectra of extragalactic objects. *Publications of the Astronomical Society of the Pacific*, 93:5–19, February 1981. doi: 10.1086/130766.

[14] P. N. Best, G. Kauffmann, T. M. Heckman, and Ž. Ivezić. A sample of radio-loud active galactic nuclei in the Sloan Digital Sky Survey. *Monthly Notices of the Royal Astronomical Society*, 362(1):9–24, September 2005. doi: 10.1111/j.1365-2966.2005.09283.x.

[15] J. J. Condon and Cotton. The NRAO VLA Sky Survey. *The Astronomical Journal*, 115(5):1693–1716, May 1998. doi: 10.1086/300337.

[16] Robert H. Becker and White. The FIRST Survey: Faint Images of the Radio Sky at Twenty Centimeters. *The Astrophysical Journal*, 450:559, September 1995. doi: 10.1086/176166.

[17] M. Vitale and Zuther. Classifying radio emitters from the Sloan Digital Sky Survey. Spectroscopy and diagnostics. *Astronomy & Astrophysics*, 546:A17, October 2012. doi: 10.1051/0004-6361/201219290.

[18] Z. S. Yuan, J. L. Han, and Z. L. Wen. Radio luminosity function of brightest cluster galaxies. *Monthly Notices of the Royal Astronomical Society*, 460(4):3669–3678, August 2016. doi: 10.1093/mnras/stw1125.

[19] P. Oliva-Altamirano and Brough. Galaxy And Mass Assembly (GAMA): testing galaxy formation models through the most massive galaxies in the Universe. *Monthly Notices of the Royal Astronomical Society*, 440(1):762–775, May 2014. doi: 10.1093/mnras/stu277.

[20] L. Woltjer. Emission Nuclei in Galaxies. *The Astrophysical Journal*, 130:38, July 1959. doi: 10.1086/146694.

[21] C. Megan Urry and Paolo Padovani. Unified Schemes for Radio-Loud Active Galactic Nuclei. *Publications of the Astronomical Society of the Pacific*, 107:803, September 1995. doi: 10.1086/133630.

[22] Z. L. Wen and J. L. Han. Dependence of the bright end of composite galaxy luminosity functions on cluster dynamical states. *Monthly Notices of the Royal Astronomical Society*, 448(1):2–8, March 2015. doi: 10.1093/mnras/stu2722.

[23] Scott D. Tremaine and Richstone. A test of a statistical model for the luminosities of bright cluster galaxies. *The Astrophysical Journal*, 212: 311–316, March 1977. doi: 10.1086/155049.

[24] L. P. David, P. E. J. Nulsen, B. R. McNamara, W. Forman, C. Jones, T. Ponman, B. Robertson, and M. Wise. A high-resolution study of the hydra a cluster with chandra: Comparison of the core mass distribution with theoretical predictions and evidence for feedback in the cooling flow. *The Astrophysical Journal*, 557(2):546, aug 2001. doi: 10.1086/322250. URL `https://dx.doi.org/10.1086/322250`.

[25] Christopher J. Miller and Nichol. The C4 Clustering Algorithm: Clusters of Galaxies in the Sloan Digital Sky Survey. *The Astronomical Journal*, 130(3):968–1001, September 2005. doi: 10.1086/431357.

[26] Guinevere Kauffmann and Heckman. The host galaxies of active galactic nuclei. *Monthly Notices of the Royal Astronomical Society*, 346(4): 1055–1077, December 2003. doi: 10.1111/j.1365-2966.2003.07154.x.

[27] L. J. Kewley and Dopita. Theoretical Modeling of Starburst Galaxies. *The Astrophysical Journal*, 556(1):121–140, July 2001. doi: 10.1086/321545.